A Coupled Memcapacitor Emulator Based Relaxation Oscillator

Dongsheng Yu, *Member, IEEE*, Zhi Zhou, Herbert H.C. Iu, *Senior Member, IEEE*, Tyrone Fernando, *Senior Member, IEEE*, and YiHua Hu

Abstract—**This paper proposes a floating emulator circuit for mimicking the dynamic behaviors of flux coupled memcapacitors (MCs) by making use of common off-the-shelf active devices. The equivalent constitutive relation of the coupled MC emulators is theoretically presented in details. The coupled MCs are then utilized to structure new relaxation oscillators (ROs) with the purpose of achieving controllable oscillation frequency and duty cycle. In consideration of different parameter configuration cases, an experimental investigation is carried out using a practical circuit emulating the dual coupled MCs and the ROs. Good agreement between experimental and theoretical results confirms that dual coupled MCs can be utilized to structure ROs with high controllability.**

Index Terms—Memcapacitor emulator, coupling, relaxation oscillator.

I. INTRODUCTION

MEMCAPACITOR (MC) is a newly generalized energy storage element based on the conception of memristor (MR) [1], [2]. To date, tremendous effort has been put into examining the inherent characteristics and developing potential applications of MCs. Their abilities of processing and storing information without the requirement of power source would open up new realms for future circuit investigations and applications in a range of areas including non-volatile memories, low-power computation, biological systems, oscillators, filters, and so on [2]-[7].

Although micro-scale devices with memcapacitive effects have been achieved [8], [9], solid MC devices are currently still not well popularized. Hence, various emulating methods have been recently proposed to analyze their equivalent dynamical characteristics and potential applications. Based on the constitutive relation, behavioral models of MC system have been established by using PSPICE simulation [10]. Several circuit mutators for emulating MC have been also proposed in [11-13] by taking advantages of active devices and MRs. MC emulators in serial, parallel, hybrid and even complicated Wye

and Delta connections with multiple input sources are proposed on the basis of an expandable MR emulator [14]. MC emulators which can be implemented by practical off-the-shelf electronic components are exhibited in [15-17]. However, most of these earlier reported emulators have the restriction of one terminal connected to the ground. Inspired by the mutators for transforming MR into floating MC, as conceptually discussed in [18], a floating MC emulator was recently proposed and experimentally tested in [19]. Interestingly, by pointing out that most of the existing MC emulators are designed necessarily based on MR, a new set of MR-less MC emulator was proposed in [20]. Very recently, a method for emulating floating MCs with piecewise-linear constitutive relations is presented based on multiple-state floating capacitor in [21]. Undoubtedly, these emulators have assisted researchers in discovering the dynamic behaviors of MC elements.

The MC based oscillator is an attractive topic recently emerging in nonlinear electronic systems. A new resistive-less relaxation oscillator (RO) is proposed by making use of two MCs as well as one capacitor and one MC in serial [22], of which the necessary conditions for oscillating are introduced and the generalized closed-form expression of the oscillation frequency is derived. As further described in [23], Joglekar's window function is adopted for interpreting the nonlinear boundary characteristics of a charge-controlled MC. Also, the dynamic behaviors and necessary oscillation conditions of the MC based RO are theoretical analyzed in details. It has been proved that, nonlinear MCs are also capable of being utilized to construct chaotic oscillators [24], [25]. The analysis results of [24] show that, in addition to chaotic oscillation, typical period-doubling bifurcations and period-3 windows can also be observed in the nonlinear MC based oscillator.

Recently, coupling is disclosed as the third relation beyond series and parallel connections of memristive circuits in [26], of which the mechanical dynamic coupling of MCs is taken into account for illustration purpose. Also, both the theoretical and experimental results reported in [27] reflect that the dynamic characteristics of two coupled MRs highly depend on the coupling strength and connection polarities. Hence, it can be speculated that coupled MCs could provide us more opportunities for developing new electronic devices with unique functions. However, very few works currently focus on the practical implementation of coupled MC emulators and its possible application in electronic circuits.

In this letter, a practical emulator of coupled MC is newly proposed and then used for structuring ROs, of which the output oscillation period and duty cycle can be purposefully

controlled in virtue of the coupling action.

II. DESIGN OF THE COUPLED MC EMULATOR

The proposed schematic of dual coupled MC emulator is depicted in Fig.1. One op amp, one multiplier and four current feedback op amps (CFOA) are necessarily required for building each emulator, MC1 or MC2. The upper MC emulator encircled by red frame is first taken as demonstration for interpreting the equivalent memcapacitance. According to the operational function of CFOA AD844, we have

$$v_{u11} = \frac{R_{21}}{R_{11}} v_{A1B1} , \qquad (1a)$$

$$v_{u31} = -\frac{1}{R_{11}C_1} \varphi_{A1B1} , \qquad (1b)$$

where φ_{A1B1} is the time integral of terminal voltage v_{A1B1}. v_{u11} and v_{u31} are the output voltages of CFOAs U11 and U31, respectively. The coupling action is achieved by two adder circuits structured by op amps U51 and U52. The output voltage of op amp U51 can be calculated by

$$v_{u51} = \frac{R_{51}}{R_{31}R_{11}C_1} \varphi_{A1B1} - \frac{R_{51}}{R_{41}} v_{s1} - \frac{R_{51}}{R_{c1}} v_{u32} . \qquad (2)$$

By referring to the datasheet of AD633JN, v_{w1} can be derived by

$$v_{w1} = v_{u51} \cdot v_{u11} \frac{R_{61} + R_{71}}{10R_{61}} . \qquad (3)$$

Based on the actions of U21 and U41, the current i_{MC1} going through terminals A_1 and B_1 is in fact decided by voltage v_{w1}. Therefore, we have

$$i_{MC1} = C_{1m} \frac{dv_{w1}}{dt} , \qquad (4a)$$

$$q_{MC1} = C_{1m}v_{w1} , \qquad (4b)$$

where q_{MC1} is the time integral of i_{MC1}. Likewise, the voltage v_{u32} inputted from MC2 can be calculated by $-\varphi_{A2B2}/R_{12}C_2$, of which φ_{A2B2} is the time integral of voltage v_{A2B2}. Hence, the memcapacitance of MC1 can be derived by considering the coupling action,

$$C_{M1}(\varphi_{A1B1}, \varphi_{A2B2}) = \frac{q_{MC1}}{v_{A1B1}} = \alpha_1 \varphi_{A1B1} + \beta_1 + k_2 \varphi_{A2B2} . \qquad (5)$$

Likewise, the memcapacitance of MC2 can be expressed by

$$C_{M2}(\varphi_{A2B2}, \varphi_{A1B1}) = \frac{q_{MC2}}{v_{A2B2}} = \alpha_2 \varphi_{A2B2} + \beta_2 + k_1 \varphi_{A1B1} . \qquad (6)$$

where k_1 and k_2 denote the coupling strength between MC1 and MC2. With respect to (5) and (6), the values of coefficients α_1, α_2, β_1, β_2, k_1 and k_2 can be calculated by

$$\alpha_1 = \frac{\xi_1}{R_{11}R_{31}C_1} , \beta_1 = -\frac{\xi_1}{R_{41}} v_{s1} , k_1 = \frac{\xi_2}{R_{11}R_{c2}C_1} , \qquad (7a)$$

$$\alpha_2 = \frac{\xi_2}{R_{12}R_{32}C_2} , \beta_2 = -\frac{\xi_2}{R_{42}} v_{s2} , k_2 = \frac{\xi_1}{R_{12}R_{c1}C_2} , \qquad (7b)$$

where

$$\xi_1 = \frac{R_{21}R_{51}(R_{61} + R_{71})C_{1m}}{10R_{11}R_{61}} , \qquad (8a)$$

$$\xi_2 = \frac{R_{22}R_{52}(R_{62} + R_{72})C_{2m}}{10R_{12}R_{62}} . \qquad (8b)$$

It can be seen from (7) that the coupling strength can be easily adjusted by tuning the values of resistors R_{c1} and R_{c2}. Note that, although the coupling action achieved via flux is supposed to be wireless, the coupling interaction between MC1 and MC2 of the proposed emulator is implemented by hardware wire instead in comprehensive consideration of implementation simplicity and emulation performance.
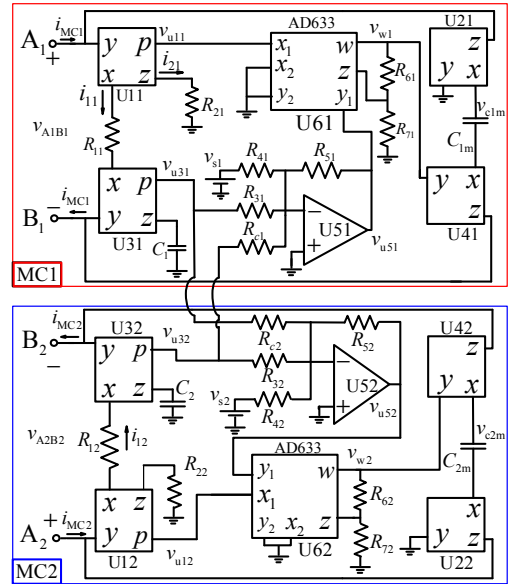

Fig.1 Dual coupled MC emulator

III. ANALYSIS OF COUPLED MCS BASED RELAXATION OSCILLATORS

Two cases of ROs structured by coupled MC emulator are exhibited in Fig.2. Two Zener diodes are connected between ground and the output terminal of each RO to restrict the output voltage amplitudes, V_{OH} and $-V_{OL}$. In Fig.2 (a), MC1 is utilized to structure RO1 and an independent external voltage v_{o2} is applied to MC2. The voltage v_{f1} between R_{p2} and R_{p3} possesses only two possible threshold values, V_h and V_l, namely, $V_h = R_{p3}V_{OH}/(R_{p2}+R_{p3})$ and $V_l = -R_{p3}V_{OL}/(R_{p2}+R_{p3})$. It can be deduced that, the voltage across MC1 is timely varied between V_h and V_l and the following equations hold,

$$q_{MC1} = C_{M1}v_{A1B1} , \qquad (9a)$$

$$i_{MC1} = v_{A1B1}\frac{dC_{M1}}{dt} + C_{M1}\frac{dv_{A1B1}}{dt} = \frac{v_{o1} - v_{A1B1}}{R_{p1}} . \qquad (9b)$$

where v_{o1} is the output oscillation voltage and equal to either V_{OH} or V_{OL}. Based on (9a) and (9b), the set of system equations

for describing RO1 can be expressed by

$$
\begin{cases}
\dfrac{dv_{A1B1}}{dt} = \dfrac{v_{o1} - v_{A1B1} - R_{p1}k_1 v_{A2B2} v_{A1B1} - R_{p1}\alpha_1 v_{A1B1}^2}{R_{p1}(\alpha_1 \varphi_{A1B1} + \beta_1 + k_2 \varphi_{A2B2})} \\
\dfrac{d\varphi_{A1B1}}{dt} = v_{A1B1}, \dfrac{d\varphi_{A2B2}}{dt} = v_{A2B2}
\end{cases} , \quad (10)
$$

For the special case of $v_{A2B2}=0$, MC1 is independently operated and RO1 can be self excited without the coupling influence from MC2. Hence, we have

$$
\begin{cases}
\dfrac{dv_{A1B1}}{dt} = \dfrac{v_{o1} - v_{A1B1} - R_{p1}\alpha_1 v_{A1B1}^2}{R_{p1}(\alpha_1 \varphi_{A1B1} + \beta_1)} \\
\dfrac{d\varphi_{A1B1}}{dt} = v_{A1B1}
\end{cases} . \quad (11)
$$

It can be seen that (11) possesses high nonlinearities and can hardly be analytically solved. However, the voltage v_{A1B1} across MC1 can still be calculated by numerical algorithms. During the time interval of $v_{o1}= V_{OH}$, MC1 is charged and v_{A1B1} is nonlinearly increased from V_l to V_h, while for the time interval of $v_{o1}= V_{OL}$, MC1 is discharged and v_{A1B1} is nonlinearly reduced from V_h to V_l. Hence, the voltage v_{A1B1} is repeatedly varied with identical period as the output voltage v_{o1}. For the case of $v_{A2B2}\neq0$ but a time-variant voltage, the output oscillation behaviors of RO1 will be unavoidably influenced by MC2 via the coupling action, as shown by (10).
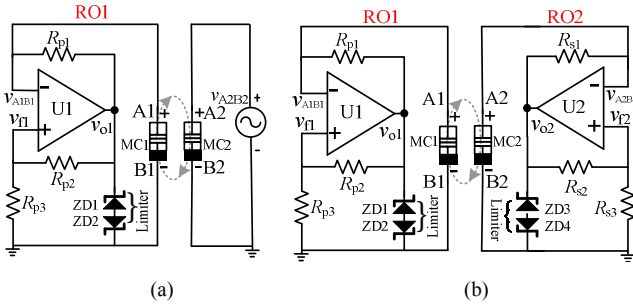

Fig.2 Coupled MC based relaxation oscillators (a) case 1 (b) case 2

By replacing voltage source v_{A2B2} with another RO circuit, two parallel ROs (RO1 and RO2) with the abilities of self excitation and controllability can be achieved, as shown in Fig. 2(b). The set of system equations for describing the coupled ROs can be rewritten by

$$
\begin{cases}
\dfrac{dv_{A1B1}}{dt} = \dfrac{v_{o1} - v_{A1B1} - R_{p1}k_1 v_{A2B2} v_{A1B1} - R_{p1}\alpha_1 v_{A1B1}^2}{R_{p1}(\alpha_1 \varphi_{A1B1} + \beta_1 + k_2 \varphi_{A2B2})} \\
\dfrac{d\varphi_{A1B1}}{dt} = v_{A1B1} \\
\dfrac{dv_{A2B2}}{dt} = \dfrac{v_{o2} - v_{A2B2} - R_{p2}k_2 v_{A1B1} v_{A2B2} - R_{p2}\alpha_2 v_{A2B2}^2}{R_{p2}(\alpha_2 \varphi_{A2B2} + \beta_2 + k_1 \varphi_{A1B1})} \\
\dfrac{d\varphi_{A2B2}}{dt} = v_{A2B2}
\end{cases} . \quad (12)
$$

(12) shows high complexities and the analytical expressions of v_{A1B1} and v_{A2B2} can hardly be obtained. (12) also reflects that the coupling strength k_1 and k_2 play important roles on controlling

the voltages v_{A1B1} and v_{A2B2} as well as the oscillating voltages v_{o1} and v_{o2}. For the special case of $k_1=k_2=0$, RO1 and RO2 will be operated as independent oscillators without coupling and can be described by (11). It is noted that v_{A1B1} and v_{A2B2} as well as v_{o1} and v_{o2} can be numerically calculated based on (12) and hence the oscillating frequency and duty cycle can be got with respect to given coupling strength k_1 and k_2.

IV. EXPERIMENTAL VERIFICATION

In order to validate the practical feasibility of the coupled MC based ROs, the experimental results of a hardware MC emulator and the ROs with different parameters are presented in this section. In order to comparatively analyze the hardware results, the experimental data are recorded by a TDS2014 oscilloscope and then transferred into OriginPro 8, without alteration, to draw the curves.

Without consideration of coupling action, the single emulator MC1 can be practically implemented by using circuit parameters as $R_{11}=48k\Omega$, $R_{21}=48.3k\Omega$, $R_{31}=39k\Omega$, $R_{41}=39.3k\Omega$, $R_{51}=10k\Omega$, $R_{61}=10k\Omega$, $R_{71}=88k\Omega$, $C_1=100nF$, $C_{1m}=220nF$, $v_{s1}=-15V$. The emulator circuit is supposed to possess the same dynamical characteristics as the MC. Since v_{w1} is proportional to q_{MC1} with coefficient C_{1m}, v_{w1} is sampled to characterize charge q_{MC1}. The sinusoidal voltage of $v_{A1B1}=1.9\sin(2\pi ft)V$ is imposed on the terminals of A_1 and B_1 and the measured curves according to f equal to 5, 10 and 20Hz are displayed in Fig.3. It can be seen that, the pinched hysteresis loops (PHLs) behaving as inclined "8" are together passing through origin and can be comparatively shrunk by the increment of excitation frequency. The amplitudes of v_{w1} are 7.4, 5.2 and 4.8V corresponding to these three frequencies and can be further reduced by the increment of excitation frequency.
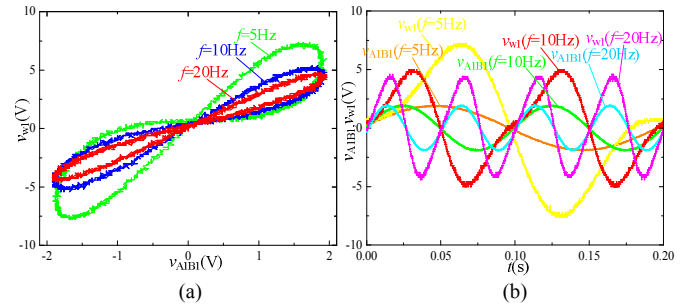

Fig.3. Experimental measurements of single MC emulator (a) PHL (b)curves of charge and voltage in time domain

The parameters used for practically implementing the coupled MCs are configured as $R_{12}=48k\Omega$, $R_{22}=48.3k\Omega$, $R_{32}=39k\Omega$, $R_{42}=39.3k\Omega$, $R_{52}=10k\Omega$, $R_{62}=10k\Omega$, $R_{72}=88k\Omega$, $C_2=100nF$, $C_{2m}=220nF$, $v_{s2}=-15V$. Two potentiometers R_{c1} and R_{c2} with maximal resistance of 1MΩ are adopted for smoothly adjusting the coupled strength. It can be calculated that the variation rates of memcapacitance are $\alpha_1=\alpha_2=1.3169uF/Wb$, and the initial memcapacitance values satisfy $\beta_1=\beta_2=94.096nF$. Two sinusoidal voltages but with different frequencies are introduced for driving this coupled MC emulator, namely, $v_{A1B1}=2\sin(40\pi t)V$ and $v_{A2B2}=2\sin(60\pi t)V$.

By setting $R_{c1}=500k\Omega$ and $R_{c2}=500k\Omega$, two MC emulators can be interacted with identical coupling strengths, $k_1=k_2=0.904uF/Wb$. The experimental results are sampled and redrawn in Fig.4 (a). Obviously, each PHL behave as an inclined "8" together passing through origin and the higher

frequency can shrink PHL in terms of the charge amplitude. For further testing, two voltages of isosceles triangle waveform with 10Hz and 20Hz frequencies are also imposed on the terminals of MC1 and MC2, respectively. The measured results are exhibited in Fig.4 (b). It can be seen that, two PHLs are also together passing through origin and PHL of MC2 under 20Hz excitation is evidently shrunk as compared with the PHL sampled from MC1. These results confirm that each emulator can provide typical memcapacitive performance even with the influence from coupling action.
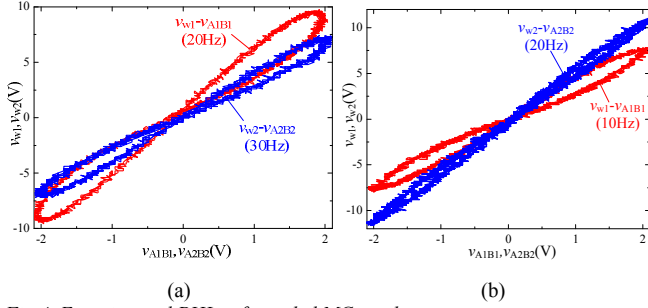

(a) (b)

Fig.4. Experimental PHLs of coupled MC emulators

The coupled MCs are then utilized to practically build the memcapacitive RO as shown in Fig.2 (a). An external excitation voltage v_{A2B2} is imposed on the terminals of MC2. Three resistors of the MC based RO are configured as $R_{p1} = 50k\Omega$, $R_{p2} = 100k\Omega$ and $R_{p3} = 28k\Omega$. Two identical Zener diodes of 1N4738 are utilized to restrict the output voltage inside the interval of [-8.2, 8.2]V. Hence, it can be analytically calculated that $V_l = -1.79V$ and $V_h = 1.79V$. For the special case of $v_{A2B2} = 0V$, the measured experimental results are displayed in Fig.5, from which we can see that, the MC1 based RO can be self-excited and outputted square voltage waveforms with stable period and duty cycle. The output voltage amplitudes are stabilized by Zener diodes at ±8.2V and the threshold voltages V_l and V_h are measured as -1.82V and 1.82V, which are very close to the calculated values. The PHL of MC1 is behaved in irregular "8" passing through origin but with nonsmooth ends, as shown in Fig.5 (b).
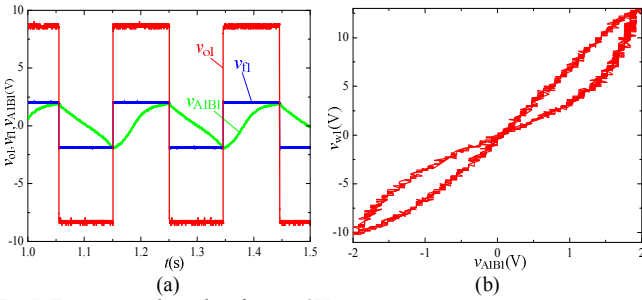

(a) (b)

Fig.5 Experimental results of $v_{A2B2}=0V$

Influences from v_{A2B2} on the oscillation behaviors of RO1 via the coupling connection are probed with respect to three cases of different excitation voltages. For case 1, a sinusoidal voltage of $v_{A2B2}=2\sin(20\pi t)V$ is adopted for comparative analysis with case 2, of which a 20Hz square voltage with 2V amplitude and 50% duty cycle is used for validation. The experimental results are presented in Fig.6(a), which discovers that the sinusoidal voltage with smaller frequency can result in smaller duty cycle

but greater oscillation period, even though the threshold voltages are maintained at the same value.

For case 3, a 20Hz square voltage with 2V amplitude but 20% duty cycle is used for comparative analysis with case 2. The measured experimental curves are exhibited in Fig. 6(b). It can be observed that, the oscillation period of RO in terms of case 2 is 221.4ms and hence bigger than 191.8ms as measured from case 3. The duty cycle of case 3 is also slightly smaller than that of case 2. This result reveals that, in addition to frequency, the duty cycle of excitation voltage also has great influences on the oscillation behaviors of RO via the coupling connection.
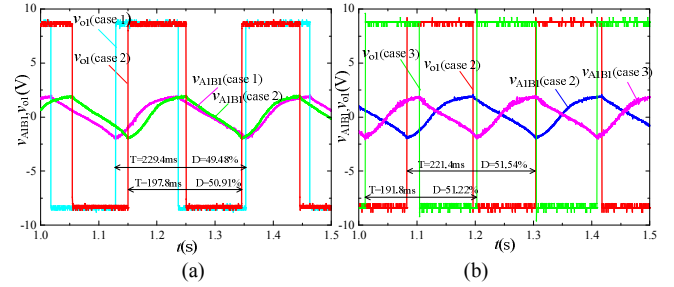

(a) (b)

Fig.6 Experimental results of coupled MC based RO (a) cases 1 and 2 (b) cases 2 and 3

Evidently, Fig.5 and Fig.6 reflect that, the output duty cycle D is no longer 50% as compared with typical RO even when $V_{OH}=V_{OL}$ and the frequency of RO1 is also decided by the parameters of voltage across MC2. Hence, the coupling action can be utilized as a new alternative method for achieving online control of coupled MC based ROs.

In accordance with Fig.2 (b), two ROs mutually interact with adjustable coupling strength in virtue of the MC emulator. The resistors for implementing the coupled ROs are configured as $R_{p1} = R_{s1} = 150k\Omega$, $R_{p2} = R_{s2} = 100k\Omega$, $R_{p3} = R_{s3} = 23k\Omega$. By setting $R_{c1}=550k\Omega$ and $R_{c2}=450k\Omega$, it can be calculated that coupling strengths satisfy $k_1>k_2$. The experimental curves are displayed in Fig.7 (a), from which we can see that PHLs of two MCs are together passing through origin but in very different shape and variation rate. Hence, it can be speculated that the variation of memcapacitance along with terminal voltage across each MC is also different from the other due to the influence from coupling action.
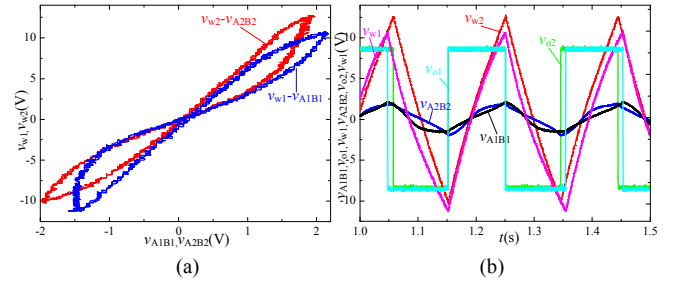

(a) (b)

Fig.7 Experimental results of coupled MC based ROs (a) PHLs (b)curves of charge and voltage in time domain

Curves of charge and voltage in time domain are given in Fig.7 (b). It can be observed that even though the threshold voltages of two MCs are identical, the equivalent charge (v_{w2} instead) of MC2 possesses bigger amplitude than MC1, and the oscillation period of RO1 is also greater than that of RO2.

Since the oscillation period of RO2 can be easily altered by the regulation of R_{s3}, then R_{s3} is configured to 17kΩ and 23kΩ respectively for comparatively analyzing the mutual influence between RO2 and RO1. As shown in Fig.8, by configuring R_{p1} =R_{s1}=150kΩ, R_{p2}=R_{s2}=100kΩ and R_{p3}=23kΩ, the output oscillating period and duty cycle of RO1 with regards to R_{s3}=17 kΩ are 184.4ms and 49.5%, respectively. For the case of R_{s3}=23 kΩ, the output period and duty cycle of RO1 are 199.8ms and 50.6%. Likewise, by altering the value of R_{p3}, the oscillation period and duty cycle of RO2 can also be regulated, as shown in Fig. 8(b). For R_{p3}=17kΩ, the output oscillating period and duty cycle of RO2 are 190.7ms and 48.4%. The output oscillating period and duty cycle of RO2 can be increased to 218.6ms and 49.4% by increasing R_{p3} to 23 kΩ. These results reveal that the both output period and duty cycle of each MC based RO can be controlled by altering the voltage across the other by making use of the coupling action. Hence, this coupled MC based ROs could offer us a new option for controlling period or duty cycle of the pulse voltage signal to an aimed value, which will provide us higher convenience in the applications of signal generator.

It is worth noting that this coupled MC emulator also has the advantages of floating terminals and can be flexibly applied in electronic circuits without grounded restriction.
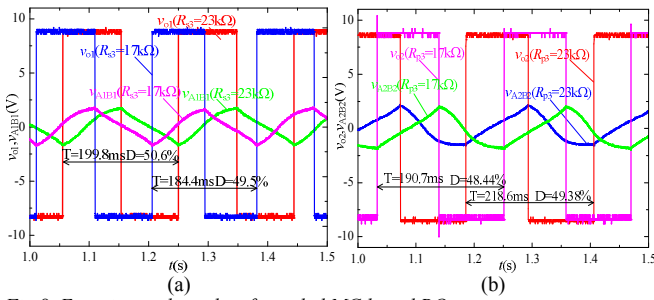

Fig.8 Experimental results of coupled MC based ROs

V. Conclusions

A new emulator capable of mimicking the dynamic behaviors of coupled MCs is proposed and utilized for the realization of RO. By taking advantages of the coupling action, oscillation period and duty cycle of the coupled MC based ROs can be purposefully controlled, which provides us a new alternative option of designing wirelessly controllable signal generators with good flexibility and practicability. Due to inherent high complexities of the coupled MC based RO, the output frequency and duty cycle are nonlinearly dependent on parameters of the coupled MCs. Hence, the controllable parameters are supposed to be properly configured in order to obtain the required output duty cycle and frequency with high accuracy.

References

[1] M. Di Ventra, Y. V. Pershin, and L. O. Chua, "Circuit elements with memory: memristors, memcapacitors and meminductors," *Proceedings of IEEE*, vol. 97, no. 10, pp. 1717–1724, Oct. 2009.

[2] L. O. Chua, "Memristor-the missing circuit element," *IEEE Transactions on Circuit Theory*, vol. CT-18, no. 5, pp. 507–519, Sept.1971.

[3] G.Y. Wang, B. Z. Cai, and P. P. Jin, "Memcapacitor model and its application in a chaotic oscillator," *Chinese Physics B*, vol.25, no.1, pp.010503, Jan. 2016.

[4] Y. V. Pershin and M. Di Ventra, "Neuromorphic, digital and quantum computation with memory circuit elements," *Proceedings of IEEE*, vol. 100, no. 6, pp. 2071-2080, Jun. 2012.

[5] C. B. Li, C. D. Li and T. G. Huang, "Synaptic memcapacitor bridge synapses," *Neurocomputing*, vol. 122, pp.370-374, Dec. 2013.

[6] J. S. Pei, J. P. Wright, M. D. Todd, S. F. Masri and F. Gay-Balmaz, "Understanding memristors and memcapacitors in engineering mechanics applications," *Nonlinear Dynamics*, vol. 80, no. 1-2, pp. 457-489, Apr. 2015.

[7] T. Driscoll, J. Quinn, S. Klein, H. T. Kim, B. J. Kim, Y. V. Pershin, M. Di Ventra, and D. N. Basov, "Memristive adaptive filters," *Applied Physics Letters*, vol.97, no.9, 093592, Aug. 2010.

[8] Y. J. Noh, Y. J. Baek, and Q. L. Hu, "Analog memristive and memcapacitive characteristics of Pt-Fe2O3 core-shell nanoparticles assembly on p(+)-Si substrate," *IEEE Transactions on Nanotechnology*, vol.14, no.5, pp. 798-805, Sep.2015.

[9] J. Flak, E. Lehtonen, M. Laiho, A. Rantala, M. Prunnila, and T. Haatainen, "Solid-state memcapacitive device based on memristive switch," *Semiconductor Science and Technology*, vol. 29, no. 10, pp. 104012, Oct.2014.

[10] D. Biolek, Z. Biolek, and V. Biolkova, "SPICE modeling of memcapacitor," *Electron. Lett.*, vol. 46, no. 7, pp. 520–522, Apr. 2010.

[11] Y. V. Pershin and M. Di Ventra, "Memristive circuits simulate memcapacitors and meminductors," *Electronic Letters*, vol. 46, no. 7, pp. 517–518, Apr. 2010.

[12] D. Biolek, V. Biolkova, and Z. Kolka, "Mutators simulating memcapacitors and meminductors," *IEEE Asia-Pacific Conference on Circuits and Systems* , pp. 800-803, Dec. 2010.

[13] D. Biolek and V. Biolkova, "Mutator for transforming memristor into memcapacitor," *Electroic Letters*, vol. 46, no. 21, pp. 1428–1429, Oct. 2010.

[14] M. P. Sah, R. K. Budhathoki, C.J. Yang, and H. Kim, "Expandable circuits of mutator-based memcapacitor emulator," *International Journal of Bifurcation and Chaos*, vol. 23, no. 5, 1330017, May 2013.

[15] X. Y. Wang, A. L. Fitch, H. H. C. Iu, and W. G. Qi, "Design of a memcapacitor emulator based on a memristor," *Physics Letter A*, vol. 376, no. 4, pp. 394–399, Nov. 2012.

[16] M. P.Sah, R. K. Budhathoki, C. Yang, and H. Kim, " Expandable circuits of mutator-based memcapacitor emulator," *International Journal of Bifurcation and Chaos*, vol.23, no.5, pp.1330017, May 2013.

[17] D. S. Yu, Y. Liang, H.H.C. Iu, L.O. Chua, "A universal mutator for transformations among memristor, memcapacitor, and meminductor" *IEEE Trans. on Circuits and Systems II-Express Briefs*, vol.61, no.10, pp.758-762, Aug. 2014.

[18] Y. V. Pershin and M. Di Ventra, "Emulation of floating memcapacitors and meminductors using current conveyors," *Electronic Letters*, vol. 47, no. 4, pp. 243–244, Jan. 2011.

[19] D. S. Yu, Y. Liang, H. Chen, and H. H. C. Iu, "Design of a practical memcapacitor emulator without grounded restriction," *IEEE Transactions on Circuits and Systems II: Express Briefs*, vol. 60, no. 4, pp. 207–211, Apr. 2013.

[20] M. E. Fouda and A. G. Radwan, "Charge controlled memristor-less memcapacitor emulator" *Electron. Lett.*, vol. 48, no. 23, pp. 1454 - 1455, Nov. 2012.

[21] D. Biolek, V. Biolkova, Z. Kolka, and J. Dobes, "Analog emulator of genuinely floating memcapacitor with piecewise-linear constitutive relation," *Circuits Systems and Signal Processing*, vol.35, no.1, pp.43-62, Jan.2016.

[22] M. E. Fouda and A. G. Radwan, "Resistive-less memcapacitor-based relaxation oscillator," *International Journal of Circuit Theory and Applications*, vol.43, no.7, pp.959-965, Jul. 2015.

[23] M. E. Fouda and A.G. Radwan, "Boundary dynamics of memcapacitor in voltage-excited circuits and relaxation oscillators," *Circuits Systems and Signal Processing*, vol.34, no.9, pp.2765-2783, Sep.2015.

[24] G. Y. Wang, B. Z. Cai, P. P. Jin, and T. L. Hu, "Memcapacitor model and its application in a chaotic oscillator," *Chinese Physics B*, vol.25, no.1, pp.010503, Jan.2016.

[25] A.L. Fitch, H. H. C. Iu, and D. S. Yu, "Chaos in a memcapacitor based circuit,"*IEEE International Symposium on Circuits and Systems (ISCAS)*, pp. 482-485, Jun.2014.

[26] W. Cai and R. Tetzlaff, "Beyond series and parallel: Coupling as a third relation in memristive systems," *IEEE International Symposium on Circuits and Systems (ISCAS)*, pp.1259-1262, 2014.

[27] D.S. Yu, H. H. C. Iu, Y. Liang, T. Fernando, and L.O. Chua, "Dynamic behavior of coupled memristor circuits," *IEEE Transactions on Circuits and Systems I, Regular Papers*, vol. 62, no. 6, pp. 1607-1616, May. 2015.